Proc. Natl. Acad. Sci. USA
Vol. 96, pp. 3154–3159, March 1999
Medical Sciences

Spatial and temporal regulation of gap junction connexin43 in vascular endothelial cells exposed to controlled disturbed flows *in vitro*

(gene regulation/gap junctional cell communication/cell proliferation/shear stress)

NATACHA DEPAOLA*, PETER F. DAVIES†, WILLIAM F. PRITCHARD, JR.‡§, LUCIO FLOREZ*, NADEENE HARBECK†, AND DENISE C. POLACEK†¶

*Department of Biomedical Engineering, Rensselaer Polytechnic Institute, Troy, NY 12180; †Institute for Medicine and Engineering, University of Pennsylvania, Philadelphia, PA 19104-3357; and ‡Laboratory of Diagnostic Radiology Research, Office of Intramural Research, National Institutes of Health, Bethesda, MD 20892

Edited by Michael A. Gimbrone, Jr., Brigham and Women's Hospital, Boston, MA, and approved December 30, 1998 (received for review October 27, 1998)

ABSTRACT **Hemodynamic regulation of the endothelial gap junction protein connexin43 (Cx43) was studied in a model of controlled disturbed flows *in vitro*. Cx43 mRNA, protein expression, and intercellular communication were mapped to spatial variations in fluid forces. Hemodynamic features of atherosclerotic lesion-prone regions of the vasculature (flow separation and recirculation) were created for periods of 5, 16, and 30 h, with laminar shear stresses ranging between 0 and 13.5 dynes/cm^2. Within 5 h, endothelial Cx43 mRNA expression was increased in all cells when compared with no-flow controls, with highest levels (up to 6- to 8-fold) expressed in regions of flow recirculation corresponding to high shear stress gradients. At 16 h, Cx43 mRNA expression remained elevated in regions of flow disturbance, whereas in areas of fully developed, undisturbed laminar flow, Cx43 expression returned to control levels. In all flow regions, typical punctate Cx43 immunofluorescence at cell borders was disrupted by 5 h. After 30 h of flow, disruption of gap junctions persisted in cells subjected to flow separation and recirculation, whereas regions of undisturbed flow were substantially restored to normal. These expression differences were reflected in sustained inhibition of intercellular communication (dye transfer) throughout the zone of disturbed flow (84.2 and 68.4% inhibition at 5 and 30 h, respectively); in contrast, communication was fully reestablished by 30 h in cells exposed to undisturbed flow. Up-regulation of Cx43 transcripts, sustained disorganization of Cx43 protein, and impaired communication suggest that shear stress gradients in regions of disturbed flow regulate intercellular communication through the expression and function of Cx43.**

Endothelial cell communication throughout the confluent monolayer as well as with circulating leukocytes and underlying smooth muscle cells plays an important role in vessel wall homeostasis and atherosclerosis (1). The localization of atherosclerotic lesions coincides with regions of disturbed blood flows where endothelial cells exhibit an altered phenotype characterized by polygonal cell shape, enhanced mitotic index, and a striking impairment of endothelial-dependent vasoresponsiveness, characteristics that have been shown to be associated with alterations in cell–cell communication (2–4). *In vitro*, fluid dynamic studies demonstrate a close relationship between flow characteristics and altered endothelial morphology and function (5–7). Taken together, *in vivo* and *in vitro* studies suggest a link between endothelial intercellular communication and hemodynamic conditions that may be relevant to focal vulnerability to atherosclerosis.

Intercellular communication occurs by a combination of humoral exchange (e.g., cytokines) and by direct transfer of signals between neighboring cells through transmembrane gap junctional assemblies composed of connexin (Cx) proteins (8). Endothelial cells express Cx40, 37, and 43, of which the most prominent connexin *in vitro* is Cx43 (9). Recently, Gabriels and Paul (10) have reported that Cx43 immunoreactivity is present at specific vascular branch points in rat aorta but absent in samples of the ventral aortic wall distant from branch points, suggesting an association between hemodynamics and Cx43 protein. However, hemodynamic characteristics were not measured nor were functional studies attempted, both measurements being difficult to undertake in the rat artery model. Disturbed flows in arteries include secondary flows, flow separation, and recirculation (11, 12). *In vitro* investigations of the effects of disturbed flow on endothelial function have demonstrated a relationship between shear stress gradients and cell proliferation (5, 6, 13), suggesting that differential forces between individual cells may compromise intercellular communication, thereby altering the normal contact inhibition of confluent endothelial monolayers. However, there have been no studies of the relationships between precisely controlled shear stresses and endothelial gap junction expression and function.

We propose that spatial gradients in fluid shear stress associated with disturbed flow regions induce local changes in endothelial gap junction-mediated intercellular communication. In this report, the spatial variations of fluid shear stresses experienced by the endothelium in areas of disturbed flow *in vivo* were modeled in a unique *in vitro* system in which precise fluid forces were spatially related to specific areas of the cell monolayer. The results demonstrate that gap junction Cx43 expression, organization, and function are regionally mapped to hemodynamic forces.

MATERIALS AND METHODS

Flow Apparatus. A parallel plate chamber was connected to a recirculating flow circuit composed of a variable-speed

The publication costs of this article were defrayed in part by page charge payment. This article must therefore be hereby marked "*advertisement*" in accordance with 18 U.S.C. §1734 solely to indicate this fact.

PNAS is available online at www.pnas.org.

This paper was submitted directly (Track II) to the *Proceedings* office.
Abbreviations: Cx43, connexin43; SSGR, shear stress gradient; GJIC, gap junctional intercellular communication.

§Present address: Hydrodynamics and Acoustics Branch, Office of Science and Technology, Center for Devices and Radiological Health, U.S. Food and Drug Administration (HFZ-132), 9200 Corporate Boulevard, Rockville, MD 20850.
¶To whom reprint requests should be addressed at: University of Pennsylvania, Institute for Medicine and Engineering, 3340 Smith Walk, Room 1072, Philadelphia, PA 19104-6383. e-mail: polacek@pobox.upenn.edu.

peristaltic pump, a fluid capacitor that damped pulsation, and a reservoir with culture medium. The flow chamber (Fig. 1) consisted of a Teflon upper plate and a stainless-steel bottom plate held together by eight screws. A medical-grade silicon gasket was used to seal the chamber and avoid fluid leakage. A precisely machined recess ($1 \times 30 \times 120$ mm) on the top plate defined the flow path in the chamber. The top plate also housed inlet and outlet ports and a quartz window for light transmission and sample visualization. The bottom plate was machined flat and polished to a mirror finish with an opening 62 mm from the flow entrance for sample placement. A rectangular step, 30-mm long, 1-mm wide, and 0.4-mm high, on the coverslip surface (located upstream from the region of interest with its largest dimension perpendicular to the flow) created a localized region of flow separation and recirculation (flow disturbance) within the chamber. The step overlapped the glass coverslip by 4 mm on each side to minimize flow-edge effects. Temperature was maintained at 37°, and pH and oxygen levels were controlled with a 95% air/5% CO_2 humidified gas mixture blown over the medium in the reservoir.

Determination of Flow Characteristics. Because the channel height in the flow chamber was much less than its width, the flow was considered two-dimensional. The fully developed channel flow, away from the step disturbance, had a uniform wall shear stress given by $\tau = 6\ \mu U/H$, where U is the mean velocity of the flow through the channel, H is the channel height, and μ is the dynamic viscosity of the fluid. In the disturbed flow region, the wall shear stress was nonuniform. The spatial variation in shear stress in regions of flow separation and recirculation was obtained from the numerical solution of the flow equations by using finite-element models. The computational domain was a two-dimensional straight channel with a rectangular step on one of the walls (Fig. 2). The aspect ratio of the step (height/width) was 0.4, and the ratio of the channel gap to the step height (H/h) was 2.5. The two-dimensional steady Navier–Stokes equations were solved by using the computational program NEKTON (14). The boundary conditions used to solve the equations were: (*i*) nonslip condition at the channel surfaces, (*ii*) a parabolic velocity profile (fully developed Poiseuille flow) assumed at the inflow, and (*iii*) at the outflow, the requirement that the same mass flow rate exited the computational domain as entered it. On the basis of these calculations, the flow velocity (U) and the medium viscosity (μ) were adjusted to produce regions of flow separation, reattachment, and flow recovery over the same endothelial monolayer at physiological levels of shear stress.

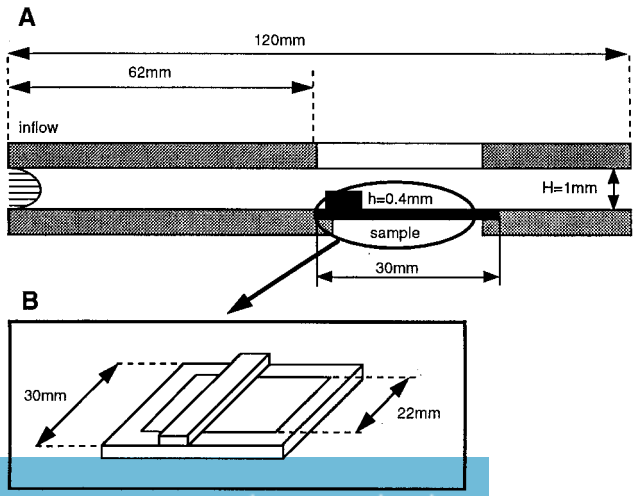

FIG. 1. (*A*) Parallel-plate flow chamber. (*B*) Glass coverslip with steel frame and surface step (flow disturbance).

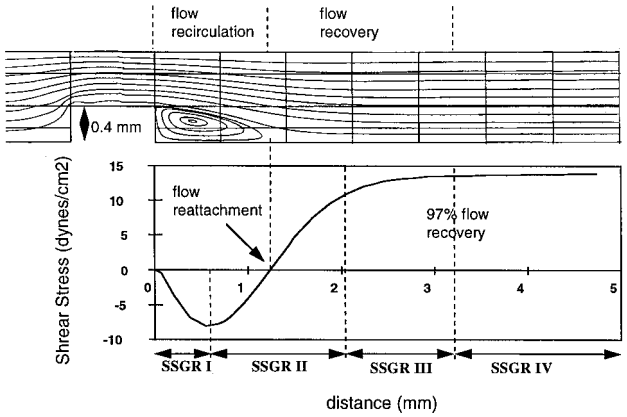

FIG. 2. Flow streamlines in the chamber showing regions of flow separation, recirculation, reattachment, and recovery. (*Lower*) The corresponding shear stress distribution on the coverslip surface. The average shear stress gradients (slope of shear stress curve) in regions SSGR I–IV are 188, 182, 22, and 0 dynes/cm^2, respectively.

Cells. Two well characterized strains of bovine aortic endothelial cells (BAEC; passages 6–8), initially isolated from

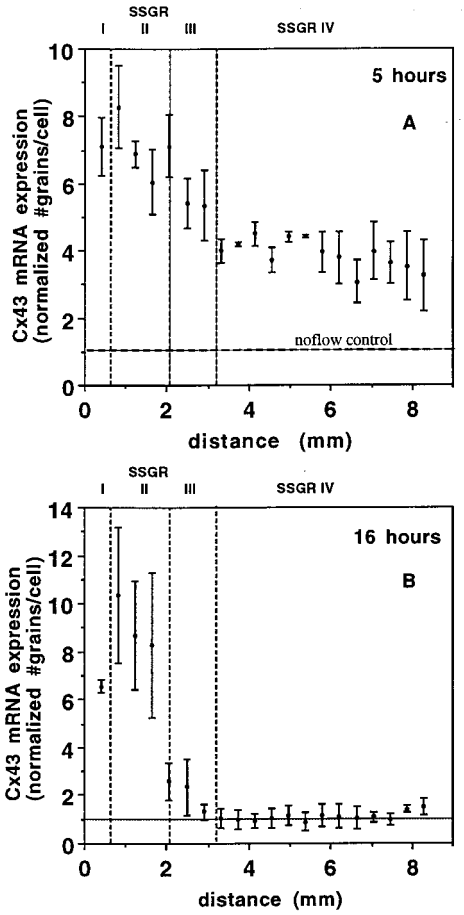

FIG. 3. Spatial distribution of Cx43 mRNA expression. (*A*) Endothelial monolayers exposed to disturbed flows for 5 h. (*B*) Endothelial monolayers exposed to disturbed flows for 16 h. Each data point represents the average number of grains per cell (normalized to the no-flow control) in three to seven high-power fields (0.21×0.15 mm) from three separate experiments. Bars = means ± SD. The horizontal axis, x (mm), is the distance measured from the downstream edge of the step. The vertical, dotted lines mark the boundaries of the four SSGRs. The shear stress gradient in SSGRI and II is 182–188 dynes/cm^2 cm. The shear stress gradient is 22 dynes/cm^2 cm in SSGRIII and negligible in SSGRIV.

yearling calf thoracic aortas, were cultured on glass coverslips that contained a fine photoetched grid (Bellco Glass), using standard techniques (15). Coverslips were coated with 0.1% gelatin, or, for *in situ* hybridization experiments, a gelatin/$CrK(SO_4)_2$ (0.5:0.05%) subbing solution was used. Monolayers were grown under static conditions in standard culture medium and transferred to the flow apparatus when confluent.

Flow Experiments. Confluent endothelial monolayers were exposed to steady disturbed flows for 5, 16, and 30 h. The viscosity of the flow medium was increased to 1.74 cP by the addition of 1 gm% dextran (M_r 5×10^5) to the standard culture medium to obtain higher wall shear stresses at relatively low fluid velocities. Previous experiments have demonstrated that dextran concentrations up to 10 gm% in culture medium are compatible with normal growth behavior and long-term viability of BAEC cultures (6). The fluid velocity through the channel was chosen to produce disturbed flow fields in which flow separation, reattachment, and recovery could be observed within a 6-mm region downstream of the surface step. The wall shear stress in the fully developed flow downstream from the flow disturbance was 13.5 dynes/cm^2. The predicted length of the recirculation region was 1.32 mm, and the absolute value of the wall shear stress within the recirculation region ranged from 0 to 8.5 dynes/cm^2.

***In Situ* Hybridization and Immunocytochemistry.** Immediately upon completion of flow exposure, coverslips were removed, rinsed briefly in buffered PBS, fixed in 4% paraformaldehyde (20 min), rinsed in PBS, dehydrated in graded alcohols, and stored desiccated and frozen at −70°C until processed for *in situ* hybridization for evaluation of Cx43 mRNA expression. cDNA was prepared from fresh rat heart total RNA, and a unique 308-bp fragment was subcloned into the RNA transcription vector Bluescript ML3+ (Stratagene) as described previously (16). Specificity of the antisense Cx43 riboprobe was demonstrated by hybridization to a single 3.0-kb Cx43-specific RNA species on Northern blots (16). Cx43 mRNA expression was visualized by using an Olympus CH30 microscope equipped with a dark-field condenser and Achromat ×20/0.40 numerical aperture objective lens.

Coverslips for immunohistochemical evaluation of Cx43 protein expression were rinsed briefly in PBS, fixed in ice-cold methanol/acetone (1:1) for 20 min, and processed immediately after fixation as described previously (16). A well characterized mouse mAb (Chemicon) directed to the C terminus of Cx43 was used.

Control cultures were plated on similar surfaces at the same time as experimental slides and maintained under no-flow conditions in a standard 37°C, humidified 95% air/5% CO_2 incubator, in the same culture medium as the experimental cultures, for the time intervals indicated. Controls were fixed and processed simultaneously with corresponding flow samples.

Dye Injections. Functional gap junctional intercellular communication (GJIC) was evaluated by microinjection of 5%

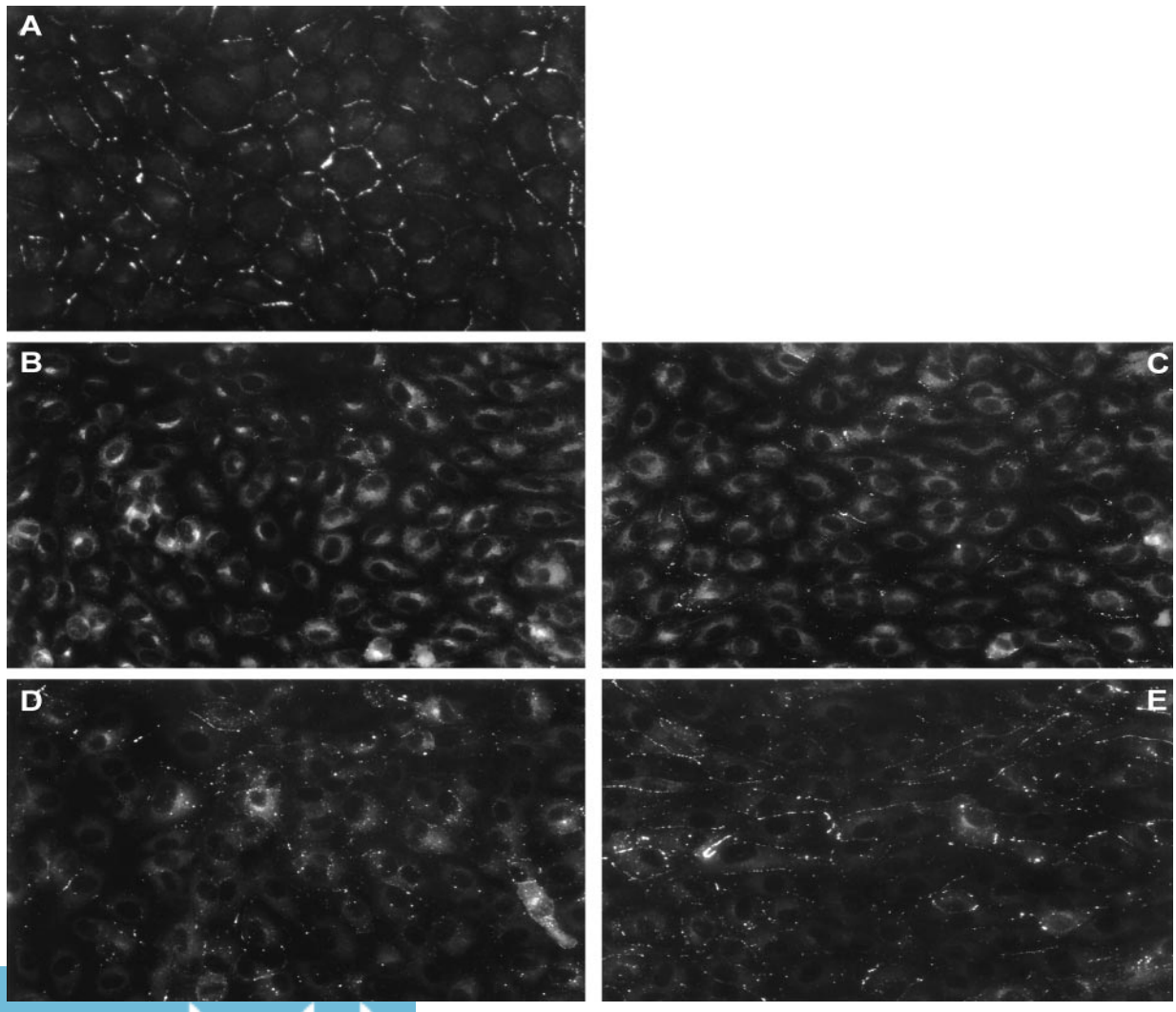

FIG. 4. Cx43 gap junction protein distribution. (*A*) No-flow control. (*B*) Five-hour SSGRI/II. (*C*) Five-hour SSGRIII/IV. (*D*) Thirty-hour SSGRI/II. (*E*) Thirty-hour SSGRIII/IV. (Bar = 10 μm.)

Lucifer yellow (M_r 457.3) and 1% tetramethylrhodamine dextran (M_r 3,000) in 0.1 M LiCl/0.05 M Tris, pH 7.8. Using an automated injection system (Eppendorf Injectman) with a fast time constant, approximately 15 cells from the recirculation area and 15 cells from the recovered flow area were injected from each flow slide. Dye injections on each flow slide were completed within 15 min from the end of the flow run. Injections were alternated between flow-recirculation regions and recovered-flow regions on each slide to achieve time matching of dye spread from pairs of injected cells. The entire time to inject 30 cells was rapid compared with the turnover of Cx43 protein (30 sec/cell or 60 sec/alternating pair). After injections, cells were fixed in 4% PFA in PBS, which cross-linked both cells and dyes. Injections and dye-spread images were recorded on Kodak TMAX 100 film using an Olympus IMT2 fluorescence-inverted microscope.

Image Analysis. Image analysis software IMAGEPRO (Media Cybernetics, Silver Spring, MD) was used to quantify the spatial variation in cellular grain density associated with Cx43 mRNA expression. Digitized images were transferred to a Pentium 166 computer using a Hitachi 3CCD HV C20 video camera and a FlashPoint (Integral Technologies, Indianapolis, IN) frame grabber. Image areas (3.2×10^{-4} cm^2) were collected at each of 20 consecutive locations (spaced 0.4 mm from each other) downstream from the edge of the step (60–140 images per sample). The average number of cells in each analyzed image was 50. To quantify Cx43 mRNA expression, matched phase-contrast and dark-field images were obtained (total of 120–280 images per sample). Ten randomly located images were chosen for analysis of no-flow control samples. Cx43 mRNA expression (number of grains per cell) at each location was quantified by evaluating the surface area occupied by the silver grains normalized by the average grain size of the sample and by the number of nuclei counted in the matching phase-contrast image.

RESULTS

Computational Results. Finite element simulation of flow (Fig. 2) demonstrated a recirculation area with a steady two-dimensional vortex downstream of the surface step (flow disturbance). The wall shear stress distribution showed an area of negative shear stress (reverse flow) coincident with flow recirculation. At the downstream boundary of the separated flow region (reattachment point) the shear stress was zero. Downstream of the stagnation point the shear stress became positive and it increased in the axial direction to a value that corresponded to fully developed downstream flow (13.5 dynes/cm^2). The predicted length of the recirculation region was 1.32 mm, and the absolute value of the wall shear stress within the recirculation region ranged from 0 to 8.5 dynes/cm^2.

As is apparent from Fig. 2, the shear stress on the coverslip surface varied over the entire disturbed flow region. The slope of the shear stress curve yielded the shear stress gradient (change in shear stress with distance). Four distinct areas of shear stress gradients (SSGRI–IV) were defined based on average values (Fig. 2). The largest gradients were located within the recirculation region and in a region extending 0.8 mm downstream of flow reattachment (regions I and II, respectively). At the downstream boundary of region II, the shear stress magnitude recovered to 80% of that in the fully developed downstream flow region, resulting in a significantly lower average SSG in region III and a negligible gradient in region IV, where the flow was fully recovered.

Connexin43 mRNA Expression in Disturbed Flow. Regional variation in endothelial Cx43 mRNA expression resulted from exposure to disturbed flow. *In situ* hybridization showed significantly greater expression of Cx43 message in SSGRI/II at both 5 and 16 h when compared with SSGRIII/IV, where grain density was increased at 5 h but returned to no-flow levels by 16 h (Fig. 3). At 5 h (Fig. 3*A*), endothelial cells exhibited a 6- to 8-fold increase in Cx43 mRNA in SSGRI/II when compared with no-flow controls. In SSGRIII/IV, a 3- to 5-fold up-regulation of Cx43 mRNA was measured. After 16 h, however, expression remained greatly elevated (8–10 times greater than no-flow controls) in SSGRI/II (Fig. 3*B*), whereas in SSGRIII/IV Cx43 mRNA expression returned to no-flow control levels. Thus, flow induced *transient* elevation of Cx43 mRNA expression in endothelial cells in regions of undisturbed flow, whereas the increase in mRNA expression was *sustained* in disturbed flow areas. Statistical analysis (*t* test) of Cx43 mRNA expression demonstrated significant differences at the $P < 0.01$ level when the pooled data from areas of high shear stress gradients (SSRGI and II) were compared with the pooled data from areas of low or negligible gradients (SSRGIII and IV) at either 5 or 16 h. There was no significant difference between control no-flow cells and recovered undisturbed flow regions (SSRGIII and IV) at 16 h. We did not evaluate in the present study whether the increased mRNA signal was a result of *de novo* synthesis and/or message stability.

Connexin43 Protein Expression. Immunocytochemical localization of Cx43 protein in endothelial cell monolayers exposed to 5, 16, and 30 h of disturbed flows were compared with matched no-flow control cultures. Control cultures exhibited a typical punctate staining of gap junction protein localized to cell–cell appositions with little intracellular immunofluorescence (Fig. 4*A*). However, after 5 h of flow, typical punctate immunoreactivity was lost largely in cells of SSGRI/II (disturbed flow region), and staining was observed

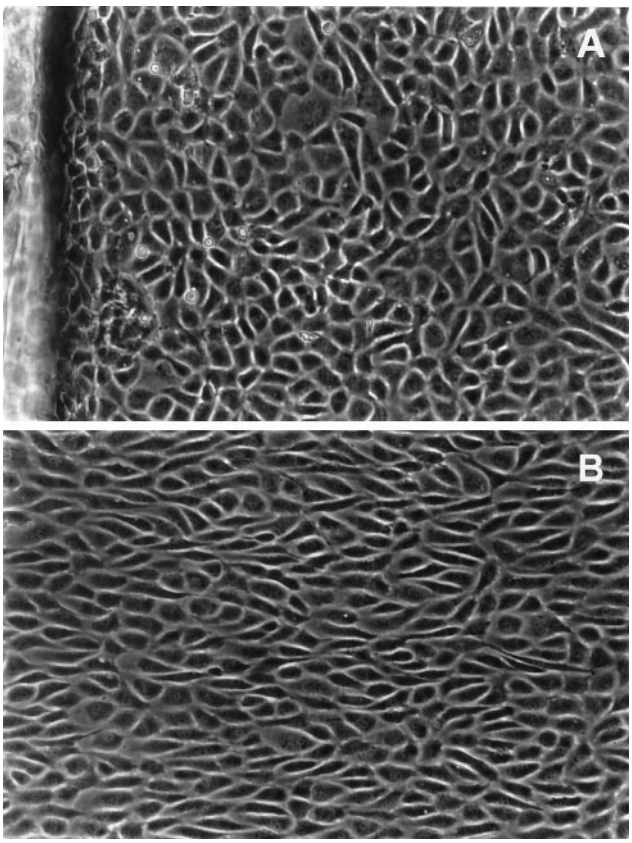

FIG. 5. Endothelial cell morphology in disturbed and undisturbed flow regions. Phase-contrast images of endothelial cells after 30-h flow. (*A*) Disturbed flow region SSGRI/II. The step is visible on the left edge of the photograph. Average cell aspect ratio (AR) was 2.4; average angle of orientation with flow direction (θ) was 40°. (*B*) Cells from the downstream recovered laminar flow region SSGRIII/IV. AR was 3.4 and θ was 15°. Flow is from left to right.

principally in the perinuclear region of the cytoplasm (Fig. 4*B*). At 5 h, SSGRIII/IV (recovered flow region) also exhibited disrupted Cx43 immunofluorescence (Fig. 4*C*). After 16 h, Cx43 immunoreactivity remained largely disrupted in the disturbed flow region, whereas in the downstream recovered flow region, punctate immunofluorescence started to reappear at cell–cell appositions (not shown). After 30 h of exposure to flow, Cx43 immunoreactivity continued to show disorganization in SSGRI/II (Fig. 4*D*), but, in contrast, within the downstream recovered flow region punctate staining was restored to cell borders (Fig. 4*E*). Note that after 30 h, whereas cells within the disturbed flow region exhibited no particular orientation of flow, endothelial cells in SSGRIII/IV had undergone significant alignment in the direction of flow (Fig. 5).

GJIC. Functional GJIC was assessed by microinjection of a mixture of dyes: Lucifer yellow (LY) (M_r 457.3), which has been shown repeatedly to pass through Cx43 gap junctions, and dextran rhodamine (M_r 3,000), which is too large to pass through the junctions and thus serves as a marker for integrity of the injected cell. After 5 h of flow, individual injected cells in SSGRI/II passed LY to 6 ± 1 neighboring cells (Fig. 6*A*). Similarly, in SSGRIII/IV, cells passed dye to 7 ± 1 neighbors (Fig. 6*B*). After 30 h of flow, however, cells from the disturbed flow region passed dye to 12 ± 2 neighbors (Fig. 6*C*) whereas within SSGRIII/IV, cells passed LY to 65 ± 4 neighboring cells (Fig. 6*D*). For reference, individual injected cells from control, no-flow cultures passed LY to an average of 38 ± 5 cells (Fig. 6*E*).

DISCUSSION

Arterial flow in regions susceptible to atherosclerosis is considered to be laminar, although extremely complex in character (17). The complexity arises from the vessel geometry and the pulsatility of blood flow, resulting in a wall shear stress distribution that varies in space and time (11, 12). Although *in vivo* studies have correlated alterations in endothelial properties with shear stress, including Cx43 protein expression (10, 18, 19), it is unclear whether the observed effects are due to the mean shear stress or to other characteristics of the hemodynamic environment, such as stress gradients, directions, and frequencies present in regions of disturbed flow. Gap junctional communication throughout the endothelium has been demonstrated in a number of studies (4, 20), with additional recent evidence for electrical and small molecule transfer to underlying smooth muscle cells (21). In attempts to study the effects of fluid flow on gap junctions *in vitro*, preliminary studies by us (22) and others (23) noted that modest levels of shear stress in laminar flow induced an increase in Cx43 mRNA expression in cultured endothelial cells. In this paper, we have addressed gene and protein expression of Cx43 and functional communication after exposure to spatially defined fluid forces in both undisturbed and controlled disturbed flow.

Sustained changes in Cx43 mRNA and protein expression were mediated by shear stress gradients rather than by shear stress alone because cells located in the downstream area of the coverslip renormalized Cx43 whereas those in the disturbed flow region, and exposed to the highest shear stress gradients, failed to do so. The reformation of Cx43 gap junctions in recovered laminar flow may be part of an ordered adaptive response to the changed hemodynamic environment. This contrasts with disturbed flow regions in which the translocation of Cx43 immunoreactivity from cell borders to intracytoplasmic locations suggested loss of a functional role for Cx43 (24, 25). The impairment of Cx43 gap junction assembly in cells

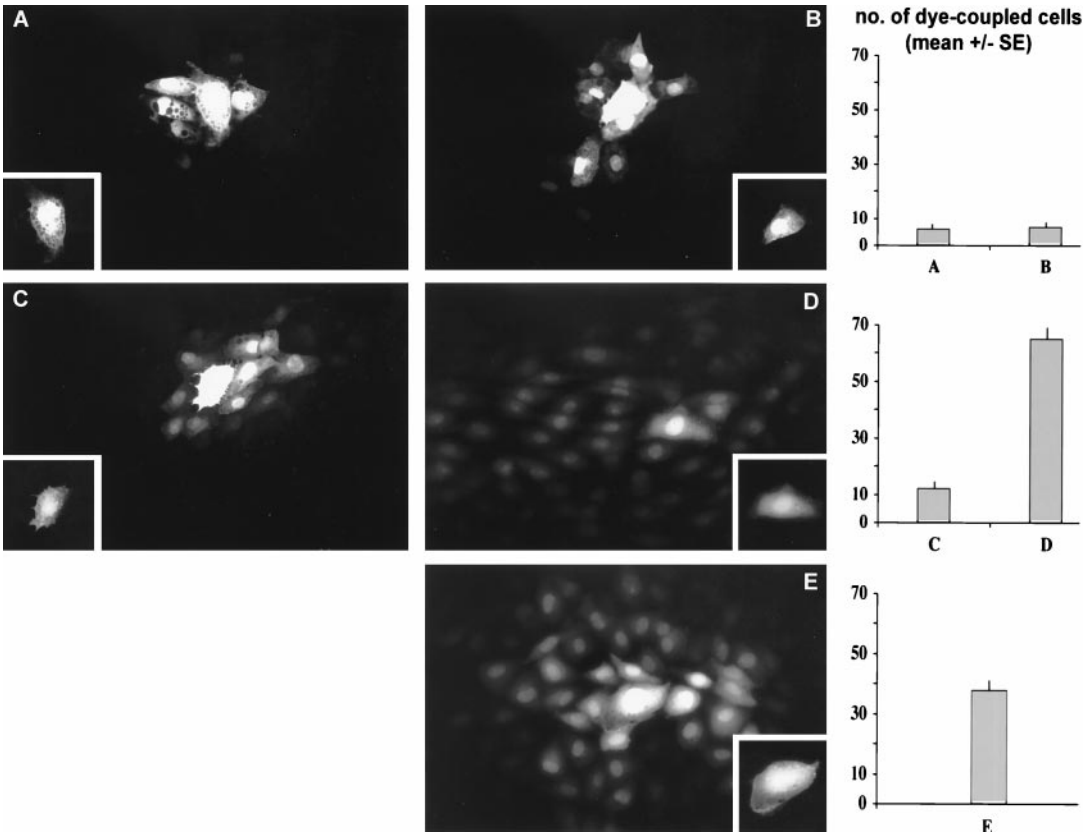

FIG. 6. Functional GJIC (dye transfer experiments). Immediately after flow exposure, cells were microinjected with a combination of dyes (see *Materials and Methods*). (*A* and *B*) Fluorescent images of representative dye spread (Lucifer yellow) within the recirculation region (SSGRI/II) and downstream recovered laminar flow region (SSGRIII/IV), respectively, after 5 h of flow. (*C* and *D*) Corresponding images after 30-h flow. (*E*) No-flow control. Each *Inset* marks the injected cell (nontransferable rhodamine dextran signal), and the extent of cell communication is shown in histogram form.

within regions of steep shear stress gradients reflects an inability to adapt, or a delay in reestablishing, intercellular communication in regions of disturbed flow as evidenced by significant differences in dye transfer between cells in regions of recirculation vs. undisturbed flow at 30 h. This controlled, quantitative study therefore suggests that there may be both structural and functional heterogeneity of intercellular communication in the arterial tree determined by local hemodynamics and, indeed, that the association of Cx43 protein expression with disturbed flow noted in the rat aorta (10) is a manifestation of this relationship.

Although there are variations of mass transfer fluxes within the region of disturbed flow, the observed increases in Cx43 mRNA expression and relocalization of Cx43 protein were not limited to the recirculation region but extended beyond it and were correlated with the magnitude of shear stress gradients. These results suggest that the observed cellular responses are modulated by the regional heterogeneity of the fluid forces on the monolayer rather than by mass transport mechanisms associated with flow recirculation.

In vivo, immunohistochemical analyses suggest that vascular endothelial gap junctional communication in large arteries is mediated primarily by Cx40 (9, 10, 27) but replaced by Cx43 protein at vascular branches and other regions predicted to be subjected to hemodynamic stresses (10). Atypical endothelial Cx43 immunostaining in the intima of atherosclerotic lesions in humans and rabbits led to the suggestion that up-regulation of Cx43 mRNA in areas of disturbed flow may be a marker for dysfunctional Cx43-mediated GJIC (16, 28). Sustained differences between hemodynamically defined regions of the endothelium *in vitro* and *in vivo* suggest that local forces significantly influence Cx43 expression and, consequently, influence gap junctional function. Compartmentalization of cell–cell communication was demonstrated clearly *in vitro* in this study; it remains to be seen whether communication is compartmentalized *in vivo*.

In summary, the present studies using a precise model of spatial flow characteristics and shear magnitude to evaluate Cx43 expression and GJIC suggest a prominent role for hemodynamics in determining regional differences in cell–cell communication that may contribute to vascular pathophysiological changes in regions of flow disturbance.

The expert technical assistance of Kyle Goldschmidt with photographic work is acknowledged. We gratefully acknowledge the support of a Whitaker Foundation Biomedical Engineering Research Grant (N.D.P.) and a National Heart, Lung, and Blood Institute HL36049 Merit Award (P.F.D.).

1. Ross, R. (1995) *Annu. Rev. Physiol.* **57,** 791–804.
2. Davies, P. F. (1995) *Physiol. Rev.* **75,** 519–560.
3. Christ, G. J. (1995) *Life Sci.* **56,** 709–721.
4. Segal, S. S. & Duling, B. R. (1987) *Circ. Res.* **61**, Suppl. II, II-20–II-25.
5. Davies, P. F., Remuzzi, A., Gordon, E. J., Dewey, C. F., Jr., Gimbrone, M. A., Jr. (1986) *Proc. Nat. Acad. Sci. USA* **83,** 2114–2117.
6. DePaola, N., Gimbrone, M. A., Jr., Davies, P. F. & Dewey, C. F., Jr. (1992) *Arterioscler. Thromb.* **12,** 1254–1257, and *erratum* (1993) **13,** 465.
7. Nerem, R. M. (1992) *J. Biomechan. Eng.* **114,** 274–280.
8. Loewenstein, W. R. (1979) *Biochim. Biophys. Acta.* **560,** 1–65.
9. Bruzzone, R., Haefliger, J.-A., Gimlich, R. L. & Paul, D. L. (1993) *Mol. Biol. Cell.* **4,** 7–20.
10. Gabriels, J. E. & Paul, D. L. (1998) *Circ. Res.* **83,** 636–643.
11. Caro, C. G., Dumoulin, C. L., Graham, J. M. R., Praker, K. H. & Souza, S. P. (1992) *J. Biomechan. Eng.* **114,** 147–149.
12. Perktold, K., Nerem, R. M. & Peter, R. O. (1991) *J. Biomechan.* **24,** 175–189.
13. Davies, P. F., Dewey, C. F., Jr., Bussolari, S. R., Gordon, E. J. & Gimbrone, M. A., Jr. (1983) *J. Clin. Invest.* **73,** 1121–1129.
14. Maday, Y. & Patera, A. T. (1989) in *State-of-the-Art Surveys on Computational Mechanics*, eds. Noor, A. K. & Oden, J. T. (Am. Soc. Microbiol., Washington, DC), pp. 71–143.
15. Gimbrone, M. A., Jr. (1976) in *Progress in Hemostasis and Thrombosis*, ed. Spaet, T. H. (Grune and Stratton, New York), pp. 1–28.
16. Polacek, D., Bech, F., McKinsey, J. F. & Davies, P. F (1997). *J. Vasc. Res.* **34,** 19–30.
17. Karino, T., Montomiya, M. & Goldsmith, H. L. (1983) in *Fluid Dynamics as a Localizing Factor for Atherosclerosis*, eds. Shettler, G., eds. Schettler, G., Nerem, R. M., Schmid-Schönbein, H., Morl, H. & Diehm, C. (Springer, Berlin), pp. 60–83.
18. Ku, D. N., Giddens, D. P., Zarins, C. K. & Glagov, S. (1985) *Arteriosclerosis (Dallas)* **5,** 293–302.
19. Okano, M. & Yoshida, Y. (1993) *Frontiers Med. Biol. Eng.* **5,** 95–120.
20. Beny, J.-L. & Gribi, F. (1989) *Tissue Cell* **21,** 797–802.
21. Beny, J. L. & Pacicca, C. (1994) *Am. J. Physiol.* **266,** H1465–H1472.
22. Polacek, D., DePaola, N., Pritchard, W. & Davies, P. F. (1995) *FASEB J.* **9,** A267.
23. Cowan, D. B., Lye, S. J. & Langille, B. L. (1998). *Circ. Res.* **82,** 786–793.
24. Peters, N. S., Coromilas, J., Severs, N. J. & Wit, A. L. (1997) *Circulation* **95,** 988–996.
25. Krutovskikh, V. A., Mesnil, M., Mazzoleni, G. & Yamasaki, H. (1995) *Lab. Invest.* **72**, 571–557.
26. Resnick, N. & Gimbrone, M. A., Jr. (1995) *FASEB J.* **9**, 874–882.
27. Bastide, B., Neyses, L., Ganten, D., Paul, M., Willecke, K. & Traub, O. (1993) *Circ. Res.* **73,** 1138–1149.
28. Polacek, D., Lal, R., Volin, M. V. & Davies, P. F. (1993) *Amer. J. Path.* **142(2),** 593–606.